Hindawi
Journal of Nanomaterials
Volume 2019, Article ID 4576135, 12 pages
https://doi.org/10.1155/2019/4576135

Research Article

A Green and Facile Approach for Synthesis of Starch-Pectin Magnetite Nanoparticles and Application by Removal of Methylene Blue from Textile Effluent

Mih Venasius Nsom,[1] **Ekane Peter Etape**,[1] **Josepha Foba Tendo**,[1] **Beckley Victorine Namond**,[1] **Paul T. Chongwain**,[1] **Mbom Divine Yufanyi**,[2] **and Nzegge William**[1]

[1]*Faculty of Science, Department of Chemistry, University of Buea, Cameroon*
[2]*Faculty of Science, Department of Chemistry, University of Bamenda, Cameroon*

Correspondence should be addressed to Mih Venasius Nsom; mihvenasius1@gmail.com

Received 9 March 2019; Revised 14 June 2019; Accepted 17 July 2019; Published 19 August 2019

Guest Editor: Soubantika Palchoudhury

Pectin-starch magnetite hybrid nanoparticles were fabricated, characterized, and evaluated as potential absorbents for methylene blue dye based on recycling water from the textile industry. The nanocomposite adsorbent was synthesized with the iron salt coprecipitation method, and the precipitates obtained were sponge-like. The effects of a pectin : starch ratio in the absorbent and the amount of methylene blue adsorbed were investigated. The nanocomposites obtained were characterized using a Fourier-transform infrared spectroscopy (FTIR), before and after methylene blue adsorption. Fourier-transform infrared spectroscopy (FTIR) spectra provided the evidence that the starch-pectin iron oxide hybrid nanoparticles were successfully synthesized. It also indicated that the hybrid nanoparticles actually absorbed the methylene blue dye from the effluent. PXRD results showed that the synthesized hybrid composite adopted the spinel microstructure of Fe_3O_4 though the crystallinity of the composite decreased with an increase in the pectin : starch ratio. Furthermore, calculations based on PXRD showed that the synthesized powders were nanoparticles. The amount of adsorbed dye by hybrid adsorbent increased with an increase in the starch : pectin ratio, and the increase was better observed at a low polymer concentration of 18%. The amount of adsorbed dye by hybrid adsorbent was high at high pH and low at low pH value which attested to the ion exchange and electrostatic force mechanism during the adsorption process. Finally, the capacity of the absorbent decreased with an increase in temperature.

1. Introduction

Day-to-day human activities (domestic and industrial) influence the flow, storage, and quality of available fresh water. Industries have a large potential to cause lake, stream, and river pollution. The nature of pollution varies from one industry to another and from one plant to another [1]. Dye-containing wastewaters from the textile industry are an important cause of severe pollution problems worldwide [1]. Effluents containing dyes are usually coloured, and the breakdown products of dyes are toxic as well as carcinogenic or mutagenic by virtue of the presence of benzidine, naphthalene, and other aromatic compounds [1]. High concentrations of textile dyes in water bodies reduce the reoxygenation capacity of the receiving water and cut off sunlight thereby upsetting biological activities such as photosynthesis in aquatic organisms. Toxicity and mutagenicity of synthetic dyes have increasingly become a major occupational hazard and challenge with regard to their use and safety in the textile industry [2]. Textile printing and dyeing industries such as Cotonniere Industrielle du Cameroun (CICAM) in Douala, Cameroon, are water-intensive and require large volumes of freshwater at various steps of printing which lead to the release of large volume of wastewater. The wastewater, if treated, can be recycled into the industries and the neighboring communities. The effluents from the wastewater usually

contain suspended solids such as azoic, indigo and aniline, bleaching agents, salts, acids/alkalis, and heavy metals and have a high biological oxygen demand (BOD) and chemical oxygen demand (COD) [3]. The first contaminant to be recognized in such wastewater is colour. The presence of small amounts of dyes in water is very visible and undesirable. Thus, the decolourisation of wastewater is a major environmental concern because dyes prevent light penetration and reduce photosynthetic activities of water plants. Methylene blue is one of the commonly used dyes. On inhalation, it can give rise to short periods of rapid or difficult breathing while ingestion through the mouth produces a burning sensation and may cause nausea, vomiting, diarrhoea, and gastritis [4]. Many physicochemical methods such as adsorption, irradiation-oxidation, precipitation, and ion exchange have been used for the removal of dyes from wastewater.

Among all these physicochemical methods, adsorption is known to be the most popular technique due to the ease of operation, the comparable low-cost of application, and the high-quality of the treated effluents especially for well-designed sorption processes [5].

Activated carbon is widely used as an adsorbent (because of its high performance) for the removal of dyes from industrial wastewater [6]. However, commercially available activated carbon is very expensive, and the high cost of the method of dye removal from wastewater is a major problem to developing countries. There is therefore the need for the development of adsorbents which exhibit good adsorption capacities from locally available low-cost materials. Agricultural waste materials are cheaper and represent renewable sources [4] which have proven to be useful alternative adsorbents to high-priced commercial activated carbon. Chemical modifications have been made on some of these agricultural waste adsorbents to enhance their adsorption capacities and consequential usefulness in the treatment of wastewater [7]. Biopolymers extracted from various sources of biomass including agricultural waste have also been investigated intensively. Alginates, chitosan, and pectin have all been shown to have variable adsorption capacities [8, 9]. Their adsorption abilities are attributed to hydroxyl and carboxylate groups. These biopolymers are however highly biodegradable and do not have adequate strength and physical stability required for good adsorption. Starch is a biopolymer with hydroxyl functional groups only, and no data is available on its adsorption capacity. It can be extracted from agricultural waste in large quantities using low-cost methods. A common approach to improve the mechanical, chemical, and physical performance of biopolymers is to incorporate oxide particles which also have adsorption properties. Traditional oxides used as adsorbents include alumina, silica, and aluminosilicates [7, 10]. Recently, magnetic oxide adsorbents have attracted a lot of interest because of the possibility of using magnetic fields to facilitate the separation of adsorbent from treated waters [6]. The most important oxide particles in this regard are the superparamagnetic magnetite, maghemite, and hematite nanoparticles. However, iron-oxide nanoparticles are easily oxidised and difficult to handle. This problem has been overcome by coating the particles with more stable polymer sheaths. Biopolymers are particularly interesting because of their biocompatibility, biodegradability, and nontoxicity [11].

Chitosan, a natural polysaccharide with many useful characteristics such as hydrophilicity, antibacterial properties, and affinity for heavy metal ions, has been used to show that the covalent attachment of carboxymethylchitosan at the surface of magnetite nanoparticles through the carboxylate function makes it efficient in the fast removal of Co^{2+} and Cu^{2+} ions from aqueous solutions [12]. Coating improves the surface properties and increases stability of adsorbents. Pectin-coated iron oxide magnetic nanocomposite has been tested and proven to be an effective adsorbent for Cu (II) removal [5]. The coated iron oxide magnetic nanocomposite has been considered competent for removing different types of contaminants from water because of their high sorption, fast removal capabilities, and easy isolation methods in an aqueous medium. The nanomaterials are preferred because they have the adsorption properties of pectin and magnetic properties of iron oxide. Coprecipitation followed by its encapsulation with pectin and cross-linking with calcium ions has been employed to produce pectin-coated iron oxide magnetic nanostructured hybrid [13]. A binding method using glutaraldehyde and adipic acid has been used to synthesize pectin-iron oxide magnetic nanocomposite, and the adsorption behavior of the pectin-iron oxide magnetic adsorbent has been investigated for the removal of methylene blue from aqueous solution [5, 14]. Iron oxide-based composites are of particular interest because of the possibility to synthesize large quantities of superparamagnetic hybrid nanoparticles using a one-step facile synthetic method. Their superparamagnetism offers the possibility of using them for targeted delivery of active molecules as well as adsorbents because of the ease of separation under the influence of a magnetic field. However, low-cost ecofriendly treatment solutions that use biomass as adsorbents are of special interest. In Cameroon, there are both small and large scale operations that make use of dyes and need low cost effective adsorbents to clean their operations. Our interest in replacing either partially or wholly the pectin in the pectin-iron oxide with starch is to respond to this need. Starch is a waste product obtained from processing staple food such as cassava. Starch has the –OH functional group but not the –COOH (found in pectin), and no work has been done with a starch hybrid matrix. Our investigation seeks to establish and understand the effect of replacing pectin with starch on the structure of the nanocomposite and adsorption capacity.

2. Experimental Details

2.1. Chemicals. Hydrated ferrous chloride ($FeCl_2{\cdot}XH_2O$) from Loba Chemie PVT. LTD, Mumbai (India), hydrated ferric chloride ($FeCl_3{\cdot}6H_2O$) from J.T. Baker Chemical CO, Phillipsburb, N.J., ammonia solution from Fisons science equipment, hydrochloric acid and pectin (D-galacturonic acid) from Sigma-Aldrich, starch (native) from the Douala market, and methylene blue from Merck were of analytical grade and used without further purification.

Table 1: Variation of pectin (P) to starch (S) ratios.

Final polymer conc. (%)	P : S	Volume of pectin used (mL)	Volume of starch used (mL)	Total volume of P/S mix	Volume of Fe^{3+}/Fe^{2+} used (mL)	Volume of ammonia added (mL)	Code
0.18	1 : 2	100	200	300	60	120	MV001_NP
0.18	1 : 4	50	200	250	50	110	MV002_NP
0.18	1 : 9	30	270	300	60	120	MV003_NP
0.86	1 : 2	100	200	300	60	140	MV004_NP
0.86	1 : 4	50	200	250	50	110	MV005_NP
0.86	1 : 9	30	270	300	60	120	MV006_NP
0.86	1 : 0	20	—	20	4	50	MV007_NP

2.2. Methodology. The synthesis of the Fe_3O_4-starch-pectin-nano-hybrid composites was carried out at room temperature without purging as is usually the case with the synthesis of iron oxide nanocomposites. Methylene blue was chosen as a model dye due to its well-known characteristics such as its relative stability compared with other dyes and strong adsorption onto solids. The use of ammonia solution was for amidation of the pectin and to cause deesterification reaction at the polymer esterified group during the coprecipitation of iron ions so as to provide more binding sites for magnetite nanocomposites. The method used in this study involved the coprecipitation of two iron salts $FeCl_3{\cdot}6H_2O$ and $FeCl_2{\cdot}4H_2O$, both prepared in HCl, with the consequent addition of NH_4OH solution with vigorous stirring at room temperature [14]. The shift of the initially orange colour of the solution to black indicated the formation of magnetite particles and the reaction is illustrated in equation (1).

$$2FeCl_3(s) + FeCl_2(s) + 8NH_3(aq) + 4H_2O(s) \rightarrow Fe_3O_4(s) + 8NH_4Cl(s) \quad (1)$$

The synthesis of Fe_3O_4 using the coprecipitation method in the presence of starch/pectin mixture is expected to initiate the covalent linkage instantaneously which should prevent further particle growth, resulting in starch/pectin-coated ferrite composites with a closer control over a particle size.

2.3. Synthesis of Starch-Pectin Magnetite Nanohybrid Composites. A 10% (*w*/*v*) pectin solution was prepared by dissolving 6 g of pectin powder into hot distilled water at 60°C while stirring to ensure complete dissolution. The volume of the solution was made up to 60 mL. From the 10% pectin solution, 9 mL was measured into 500 mL volumetric flask and made up to the mark with distilled water to give a concentration of 0.18% pectin solution while a 0.86% pectin solution was prepared by measuring 17.2 mL of the 10% pectin solution into a volumetric flask and diluting with distilled water to 200 mL. A 10% (*w*/*v*) starch solution was prepared by dissolving 10 g of powder starch in 100 mL of hot distilled water at 60°C while stirring to ensure homogeneity. A 0.18% starch solution was prepared by diluting with distilled water, 13.5 mL of the 10% (w/v) starch solution to 750 mL in a capacity flask, while a 0.86% starch solution was prepared by diluting with distilled water, 51.6 mL of the 10% (w/v) starch to 750 mL in another flask. The Fe^{3+}/Fe^{2+} mixture was prepared by dissolving 31.2 g of ferric chloride in 75 ml of hot distilled water at 60°C acidified with HCl to pH 4 and stirred till complete dissolution. The solution was filtered, 12 g of ferrous chloride was added to the filtrate, and the solution was diluted to 200 mL using distilled water. 10% (*v*/*v*) ammonia solution was prepared by measuring 67.6 mL of 33% NH_3 solution into a volumetric flask and diluted with distilled water to 250 mL. Table 1 summarizes how the ratios of pectin to starch were varied.

2.4. Characterization Techniques. In order to establish the various functional groups present and the possible alterations after synthesis and methylene blue adsorption, FTIR spectra were recorded in the middle infrared (4500 cm^{-1} to 500 cm^{-1}) on Shimadzu Prestige 21 with a resolution of 4 cm^{-1} in the absorbance mode for 8 to 128 scans at room temperature. The ASCI data were plotted using OriginLab 7.0 software while the TGA were carried out using a Pyris 6 Perkin-Elmer TGA 4000-Thermal Analyzer under nitrogen atmosphere with a flow rate of 20 mL/min and temperature range of 10°C to 900°C at an increase rate of 10°C/min. The determination of the microstructure was carried out by powder X-ray diffraction measurements (PXRD). The PXRD patterns of composite were recorded on a Philips PWO4 Xpert pro X-ray diffractometer. The X-ray source was Cu-Kα with a voltage of 40 kV and a current of 30 mA. The measurement was in the scanning range of 0–80 at a scanning speed of 50 s^{-1}.

The concentrations of methylene blue solutions were analyzed by measuring their absorbance at 662 nm on a Perkin-Elmer UV/Vis spectrophotometer. This wavelength corresponds to the maximum absorption peak of the methylene blue monomer [15].

3. Results and Discussion

3.1. Appearances and Texture of Composites. The physical appearances of the synthesized composites are shown in Table 2, and the results indicated that the rigidity of the composites increased with an increase in the polymer concentration which may be attributed to intermolecular hydrogen bonds. This in effect reduces the stability of the nanopowders and a consequent reduction in the efficiency due size effect.

Table 2: Appearances of the composites synthesized.

Code	Visual inspection and other remarks on composites
MV001_NP, MV002_NP, MV003_NP	Black, loose, easy to crush, and gradually turns brownish on exposure to air
MV004_NP	Black, most gelling, strong, very difficult to crush, and remains black even after exposure to air
MV005_NP, MV006_NP	Gelling, strong, difficult to crush, and remains black even after exposure to air
MV007_NP	Gelling, strong, very difficult to crush, and remains black even after exposure to air

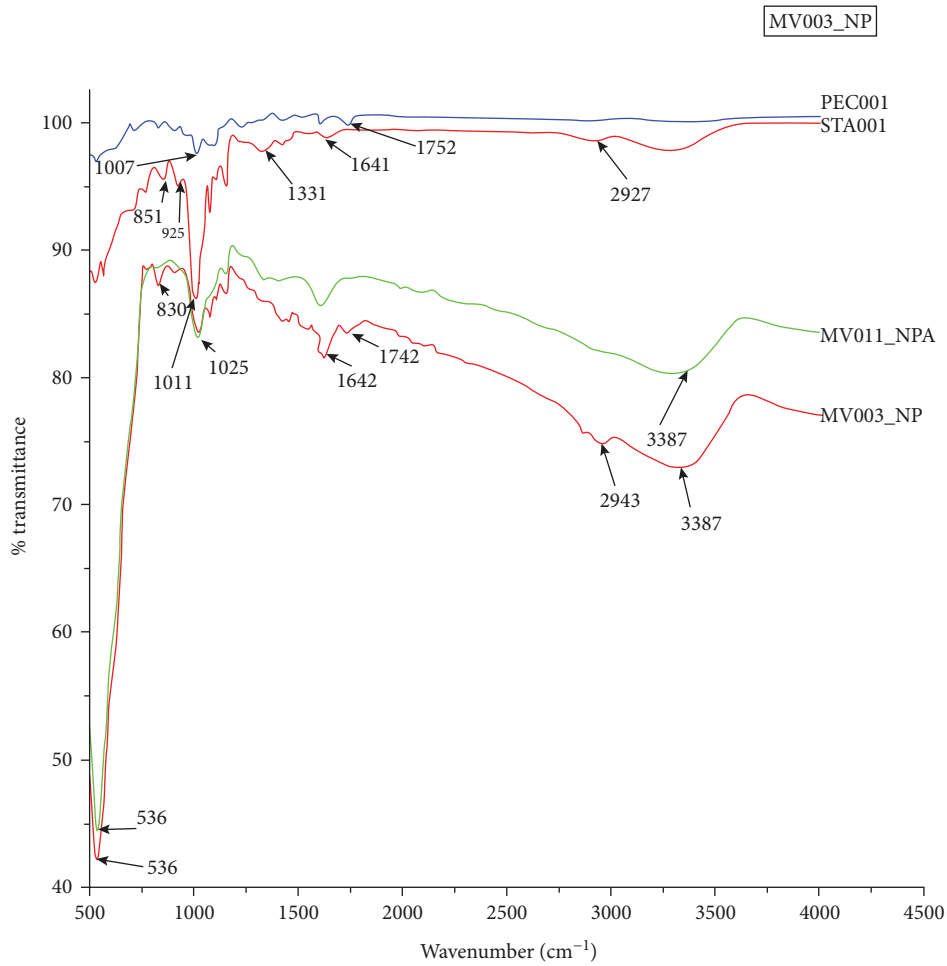

Figure 1: FT-IR spectrum of MV003_NP (composites with a starch/pectin ratio of 1 : 9 at polymer concentration of 0.18%) hybrid composites before (MV003_NP) and after (MV011_NP) adsorption.

3.2. PXRD. The PXRD patterns of the synthesized samples are shown in Figure 1. The samples MV002_NP and MV003_NP showed a diffraction peak at $2\theta = 30.2^{\circ}$, 35.5°, 43.1°, 57.0°, and 62.4° which were assigned to (220), (311), (400), (511), and (440) lattice planes of the cubic structure. Among the peaks, the diffraction at the angle $2\theta = 35.5^{\circ}$ could be attributed to Fe_3O_4, face-centered cubic structure which matched with JCPDS card no. 85 1436/JCPDS card no. 19-0629. The only crystalline peak that expressed itself in samples MV001_NP, MV004_NP, MV005_NP, and MV006_NP was the 2θ, 35.5°. This indicated that the crystallinity of the samples reduced with an increase in the polymer concentration which modified the microstructure of the iron oxide by making it more amorphous. This also indicated that there was the formation of an inverse spinel structure with a pure magnetite phase which persisted even in the presence of starch particles. The absence of any other peak demonstrated the homogeneity of the iron oxide phase.

The crystallite sizes of the composite particles were determined using Debye-Scherrer's equation which measures the size of particles according to broadening of the most intense peak (311) in the PXRD profile shown in Figure 2.

$$D = \frac{k\lambda}{\beta \cos \theta}, \tag{2}$$

where k is a dimensionless shape factor, λ is the X-ray wavelength, β is the line broadening at half the maximum intensity (FWHM), and θ is the Bragg angle.

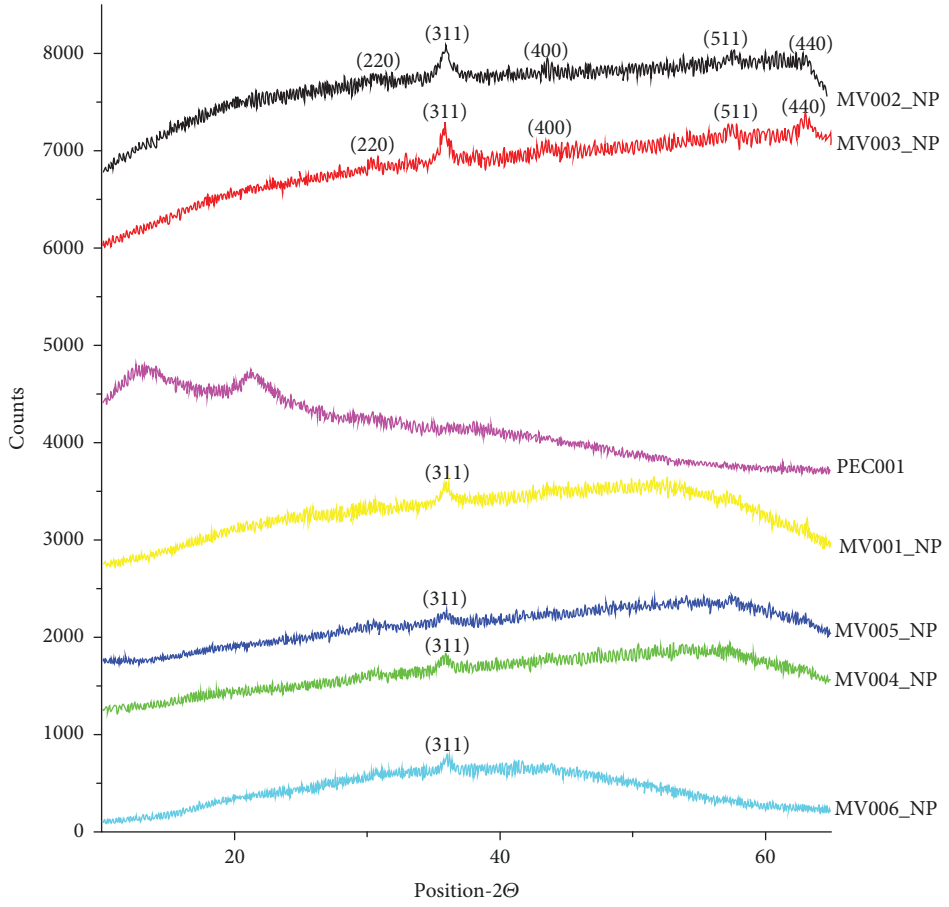

Figure 2: PXRD profiles for pectin (PEC001), composites with a starch/pectin ratio of 1 : 2, 1 : 4, and 1 : 9 at polymer concentration of 0.18% (MV001_NP, MV002_NP, and MV003_NP, respectively) and composites with a starch/pectin ratio of 1 : 2, 1 : 4, and 1 : 9 at polymer concentration of 0.86% (MV004_NP, MV005_NP, and MV006_NP, respectively).

Crystal sizes of the synthesized samples (magnetite Fe3O4) as shown in Table 3 indicated that the average particle sizes were all in the nanorange.

3.3. Fourier-Transformed Infrared (FT-IR) Spectrum Characterization. The FT-IR observed and assigned peaks are represented in Table 4 while the profiles of MV001_NP, MV002_NP, MV003_NP, MV004_NP, MV005_NP, and MV006_NP (hybrid composites before adsorption) and MV009_PN, MV010_NP, MV011_NP, MV012_NP, MV013_NP, and MV014_NP (hybrid composites after adsorption) are shown in (Figures 1, 3–7).

The spectra of PEC001 and STA001 represent the profiles of pectin and starch samples, respectively. Pectin shows peaks at 3309 cm^{-1} and 2951 cm^{-1} attributed to secondary hydroxyl groups while the one at 1750 cm^{-1} is a characteristic peak of pectin, associated with the carbonyl of the esterified pendant group [16]. The intense peak at 1011 cm^{-1} (for both PEC001 and STA001) is attributed to the glycosidic bond linking two galacturonic sugar units together. The peak at 1089 cm^{-1} is associated with the C-O stretched of secondary alcohols while the peak at 1386 cm^{-1} is assigned to the C-H bend of methyl groups. Comparison between the FTIR profiles of PEC001 (Pectin), STA001 (starch), and hybrid composites (MV001_NP, MV002_NP, MV003_NP, MV004_NP, MV005_NP, and MV006_NP) indicated the presence of new peaks at 552 cm^{-1}, 1593 cm^{-1}, and 1426 cm^{-1}. The peak at 552 cm^{-1} was attributed to the Fe-O bond vibration of Fe_3O_4 while those at 1593 cm^{-1} and 1426 cm^{-1} were attributed to the symmetric and asymmetric carboxylate-metal (COO-Fe) linkage. No changes in intensity and position of the peak at 552 cm^{-1} were recorded in the various samples which was an indication that the Fe-O bond of Fe_3O_4 was not affected during the adsorption process. The great reduction in the intensity of the peak at 1011 cm^{-1} attributed to the formation of the composites indicated that there was some interaction

Table 3: Average particle sizes.

Sample	Size (nm)
MV001_NP	10.6
MV002_NP	9.1
MV003_NP	10.2
MV004_NP	9.8
MV005_NP	9.8
MV006_NP	10.7

Table 4: Observed and assigned peaks with references indicated.

Observed peak (cm^{-1})	Assignment	Reference
1737	C=O (characteristic peak of pectin esterified pendant group)	[14]
536	Fe-O bond vibration of Fe_3O_4	[17]
1404	-CH bending of CH_2 groups	[18]
1594	Asymmetric v(C=O) vibration	[19]
2938	-CH stretching of CH_2 group vibration	[18]
1325	-CH_2 scissoring	[18]
1389 1579-1594	Symmetric and asymmetric stretching of carboxylate-metal (-COO-Fe)	[14, 19]
1074-1142	v(C-O) of -CH-OH in aliphatic cyclic secondary alcohols	[18]
1641	v(C=O) stretching vibration peak	[18]
1010-1017	C-O-C glycosidic bond linking monosaccharaides in starch and galacturonic acid in pectin	[14]
1626 and 3150	Presence of hydroxyl groups on the surface of nanoparticles	[19]

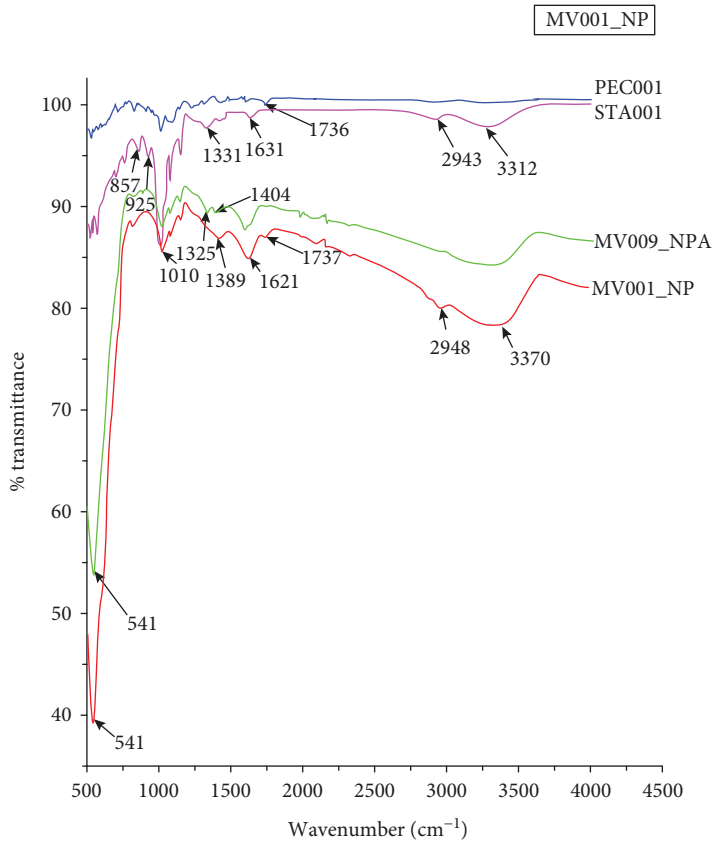

Figure 3: FT-IR spectrum of MV001_NP (composites with a starch/pectin ratio of 1 : 2 at polymer concentration of 0.18%) hybrid composites before (MV001_NP) and after (MP009_NP) adsorption.

at the level of the glycosidic bond while the reduction in peak intensity at 1742 cm^{-1}, absent in some spectra, is probably due to deesterification of the ester group along the pectin polymeric chain. The other reduction in peak intensity at 1011 cm^{-1} in all the spectra indicated an interaction of the atoms involved in the glycosidic bond with atoms of the dye.

After methylene blue adsorption, a new peak appeared at 1340 cm^{-1} and could be attributed to the Fe–S vibration which brought about the reduction in the peak intensity at 1426 cm^{-1}. Comparison between the FTIR profiles of MV001_NP, MV002_NP, and MV003_NP and hybrid composites before adsorption (MV004_NP, MV005_NP, and MV006_NP) on the one hand and hybrid composites after adsorption (MV009_PN, MP009_NP, MV010_NP, MV011_NP, MV012_NP, MV013_NP, and MV014_NP) on the other hand, as shown in Figures 1, 3–7, indicated broadening of the band with a peak at 3299 cm^{-1}. This change could be attributed to intermolecular hydrogen bonding between

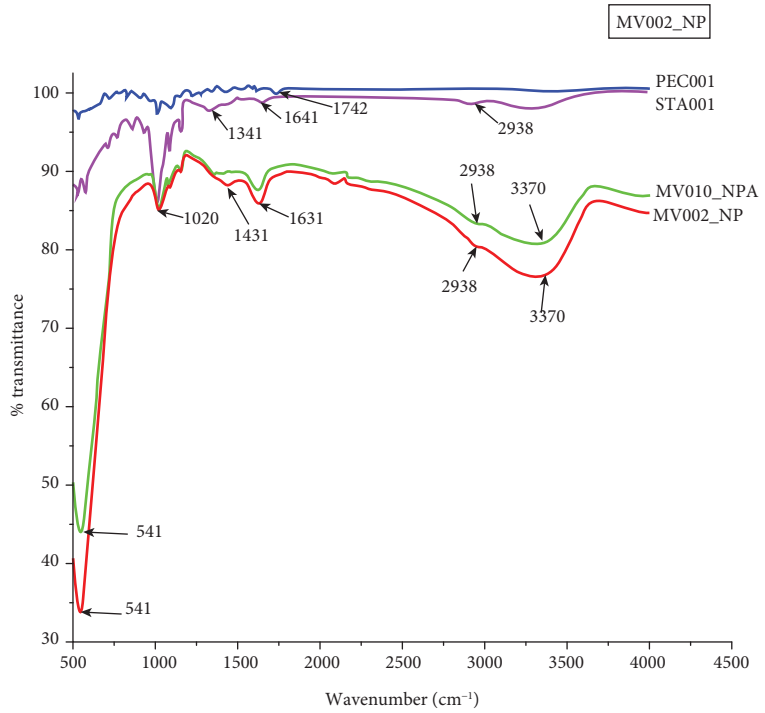

Figure 4: FT-IR spectrum of MV002_NP (composites with a starch/pectin ratio of 1 : 4 at polymer concentration of 0.18%) hybrid composites before (MN002_NP) and after (MV010_NP) adsorption.

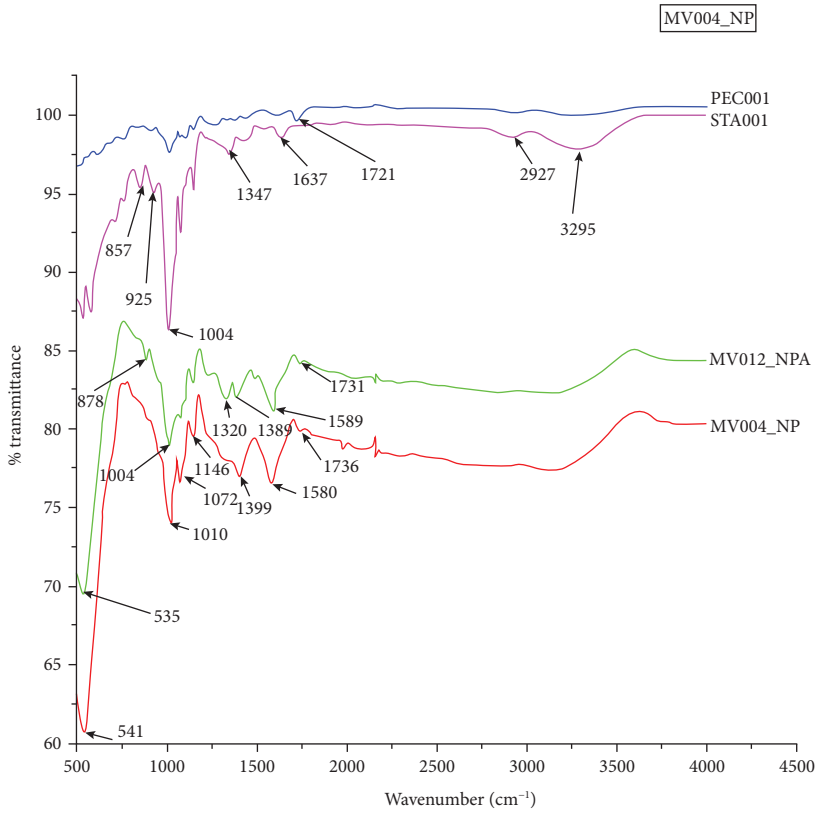

Figure 5: FT-IR spectrum of MV004_NP (composites with a starch/pectin ratio of 1 : 2 at polymer concentration of 0.86%) hybrid composites before (MV004_NP) and after (MV012_NP) adsorption.

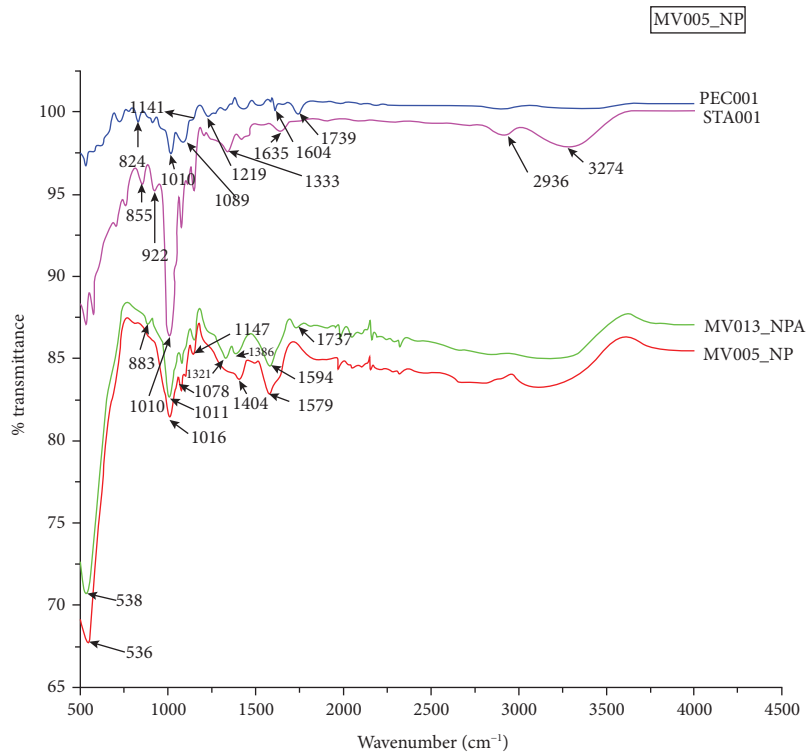

Figure 6: FT-IR spectrum of MV005_NP (composites with a starch/pectin ratio of 1 : 4 of polymer concentration of 0.86%) hybrid composites before (MV005_NP) and after (MV013_NP) adsorption.

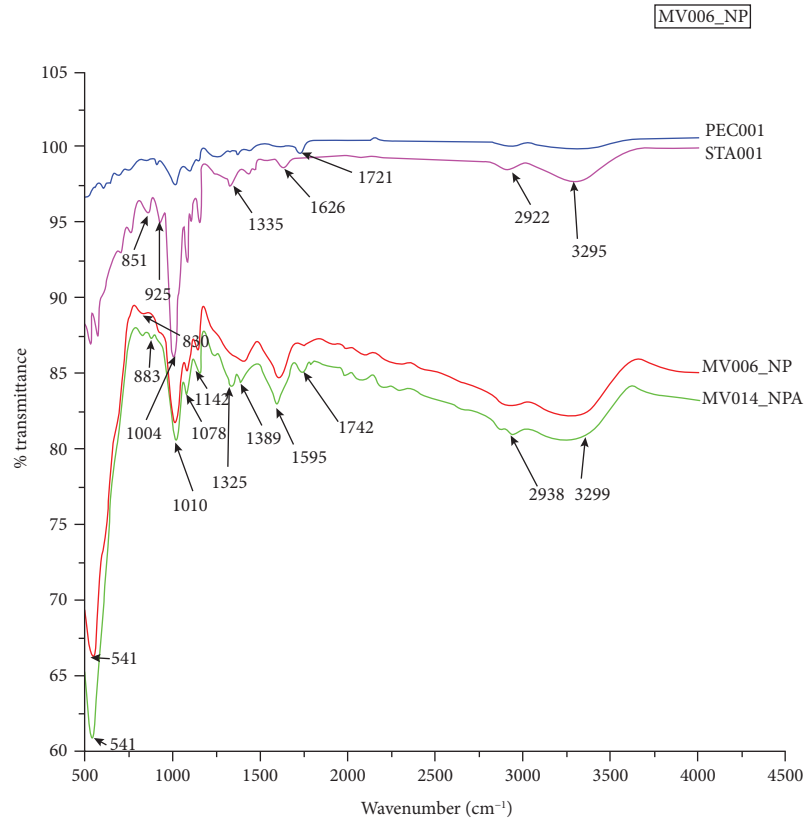

Figure 7: FT-IR spectrum of MV006_NP (composites with a starch/pectin ratio of 1 : 9 of polymer concentration of 0.86%) hybrid composites before (MV006_NP) and after (MV014_NP) adsorption.

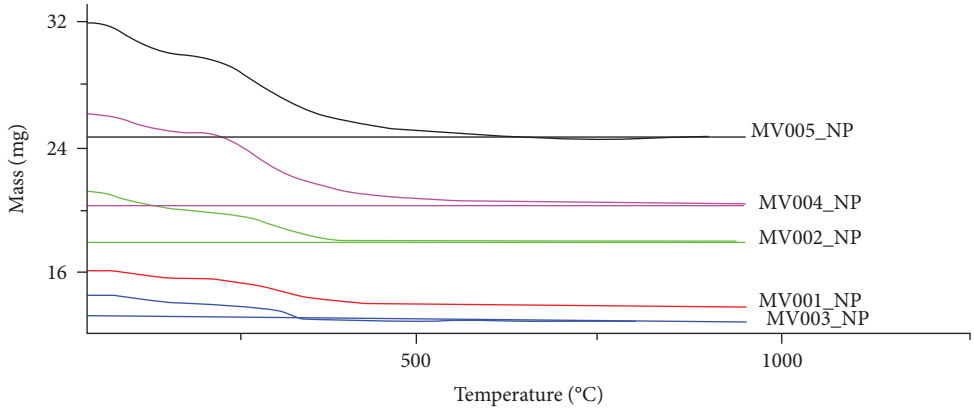

Figure 8: TGA profiles of samples (composites with a starch/pectin ratio of polymer concentration).

Table 5: Decomposition temperature and weight loss percentages.

Sample	First weight loss portion (%)	Second Wt. loss (%)	Residual Wt. (%)	Decomposition temp. (°C)
MV001_NP	2.56	9.19	88.25	375
MV002_NP	5.58	8.85	85.57	375
MV003_NP	3.44	7.64	88.92	375
MV004_NP	5.27	16.81	77.92	525
MV005_NP	7.48	15.86	76.66	525

neighboring hybrid composite and newly introduced methylene blue molecules.

The level broadening varies with the pectin : starch ratio in the hybrid composite but was indifferent to the polymer : - oxide ratio. This suggests that the adsorbent efficiency of the NPs was a function of the pectin : starch ratio in the hybrid composite.

3.4. Thermogravimetric Analysis. The TGA profiles of the hybrid pectin-starch magnetite shown in Figure 8 and weight loss percentages in Table 5 reveal two weight loss portions. The first portion at a temperature of about 102°C and corresponding to the range 2.5 - 7.5% is attributed to water of crystallization. The second weight loss portion which occurs between 250°C and 550°C corresponds to the decomposition of the hybrid with the breakage of the glycosidic bonds. The final percentage by weight of the residue which varies with the polymer concentration corresponds to iron oxide (magnetite (Fe_3O_4)) nanoparticles.

3.5. The Influence of Polymer/Oxide and Pectin/Starch Ratios and Amount of Oxide on Methylene Blue Adsorption. The variation of methylene adsorption against polymer/oxide and pectin/starch ratios and amount of oxide is shown in Table 6. The results indicated that neither the polymer : oxide ratio nor the amount of oxide present in the hybrid composite had a direct effect on the amount of methylene blue dye adsorbed. Instead, the amount of dye adsorbed by the adsorbent complex is a function of the pectin : starch ratio in the hybrid composite.

3.6. The Influence of a Pectin/Starch Ratio on Methylene Blue Adsorption. The influence of a pectin : starch ratio on methylene blue adsorption for all the samples is shown in Tables 7 and 8 and represented in Figure 9.The results revealed that the percentage of methylene blue adsorbed increased with an increase in the pectin/starch ratio. The efficiency of the absorbent reached maximum at a pectin/starch ratio of 0.50 at ambient temperature while the increase in the polymer concentration decreased the efficiency of the adsorbent which could be accounted for by the shielding effect of the constituent polymer atoms on the pores on the adsorbent.

For either polymer concentrations, 0.18 and 0.86, it was observed that a certain minimum amount of pectin was needed to maximize the adsorption of methylene blue by the adsorbents which was an indication that pectin was acting as a stabilizing agent. To determine the percentage of the dye adsorbed, the following equation was used:

$$\%\ \text{of methylene blue adsorbed} = \frac{C_o - C_f}{C_o} \times 100, \quad (3)$$

where C_o and C_f represent the initial and C_o equilibrium concentrations, respectively.

To further evaluate the percentage of methylene blue adsorbed by the pectin/starch hybrid magnetite nanocomposite, work was done with larger batches of sample and the results obtained are as presented in Table 8. These results conformed to those obtained using smaller quantities as shown in Table 7.

3.7. Influence of pH on Composite Adsorption of Methylene Blue. The results for raising the pH from 6 to 8 for MV006_NP are as shown in Table 9 and Figure 10. The

Table 6: Showing polymer/oxide and pectin/starch ratios, amount of oxide, and methylene blue adsorption.

Code	Polymer : oxide ratio	Pectin : starch ratio	Amount of Fe_3O_4 in hybrid	Methylene blue adsorption
MV001_NP	0.11	0.35	0.06	90.3
MV002_NP	0.11	0.22	0.08	44.7
MV003_NP	0.09	0.25	0.06	48.3
MV004_NP	0.22	0.48	0.09	83.3
MV005_NP	0.21	0.52	0.11	97.1

Table 7: Methylene blue adsorption by the starch-pectin magnetite nanocomposites MV001_NP, MV002_NP, MV003_NP, MV004_NP, MV005_NP, MV006_NP, and MV007_NP.

Sample	Concentration of polymer	P : S ratio	C_o	C_f	% of dye removed	% S.D.	% error
MV001_NP	0.18	0.36	25	2.43	90.3	1.53	1.70
MV002_NP	0.18	0.20	25	13.82	44.7	6.08	13.6
MV003_NP	0.18	0.22	25	12.92	48.3	3.97	8.22
MV004_NP	0.86	0.47	25	4.18	83.3	1.24	1.50
MV005_NP	0.86	0.52	25	0.72	97.1	1.04	1.07
MV006_NP	0.86	0.45	25	4.09	83.6	1.88	2.25
MV007_NP	0.86	1	25	0.31	98.7	0.64	0.65

Table 8: Results of batch trials done with larger amounts of adsorbents in larger volumes of dye solution.

Sample	Concentration of polymer	P : S ratio	C_o	C_f	% of dye removed	% S.D.	% error
MV001_NP	0.18	0.36	25	2.50	90.0	0.34	0.37
MV002_NP	0.18	0.20	25	12.04	51.8	0.25	0.49
MV003_NP	0.18	0.22	25	11.55	53.8	0.12	0.21
MV004_NP	0.86	0.47	25	4.45	82.2	0.45	0.55
MV005_NP	0.86	0.52	25	0.54	97.8	0.25	0.26
MV006_NP	0.86	0.45	25	04.66	81.3	0.33	0.41

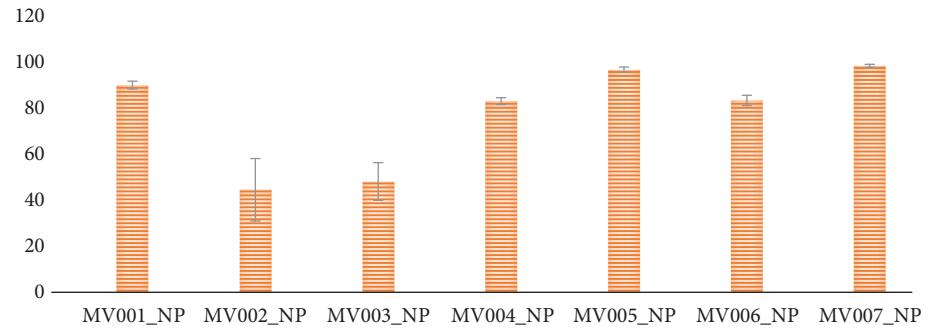

Figure 9: Bar charts showing methylene blue adsorption for various test samples.

Table 9: Influence of pH on composite adsorption of methylene blue.

Sample	pH	Standard deviation (S.D.)	Initial concentration of dye	Final concentration of dye	% adsorption of dye	% S.D.	% error
1	8	0.002	25	2.798	88.81	0.28	0.31
2	6	0.011	25	4.096	83.60	0.33	0.41

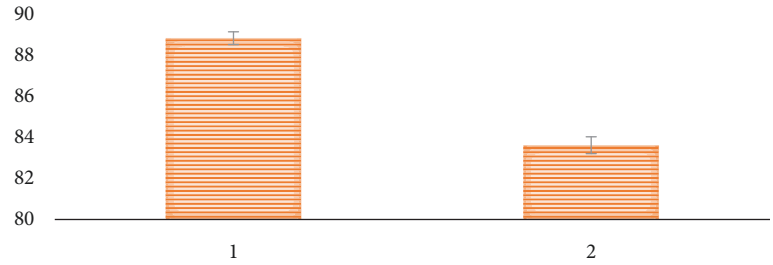

Figure 10: Bar charts showing the influence of pH on % methylene dye adsorption.

adsorption capacity of the samples increased from 83.6% to 88.81% as the pH increased from 6 to 8. Blue 1 and 2 had 100 mL of 25 mg/L of methylene blue +0.5 g of the MV006_NP sample. Methylene blue is a cationic dye, and less sorption at lower pH may be attributed to the competition of H^+ ions with methylene blue ions at sorption sites. Increasing solution pH increased the number of hydroxyl groups, thus increasing the number of negatively charged sites and enlarging the attraction between dye and adsorbent surface. Also, a net positive charge decrease with increasing pH value leads to a decrease in the repulsion between the adsorbent surface and the dye, thus improving the adsorption capacity. This means that at a higher H^+ ion concentration, the adsorbent surface becomes more positively charged, thus reducing the attraction between the adsorbent and the methylene blue ions. In contrast, as the pH increased, more negatively charged surface becomes available, thus facilitating greater dye ion uptake.

3.8. Influence of Temperature Pyrolysis on Methylene Blue Adsorption of Composite. Portions of a sample (MV002) previously heated to 60°C and 180°C were crushed and also used for the adsorption of methylene blue. The results obtained are displayed in Table 10. This was done in order to determine the effect of heat treatment on the adsorption capacity of composites.

Figure 11 shows the influence of temperature pyrolysis on methylene blue adsorption of the composite. It was noticed that the adsorption decreased with an increase in temperature. This can be explained by the fact that the nanomagnetite hybrid composite becomes unstable indicating that the critical coagulation concentration of the hybrid spinel magnetite nanoparticles correlates positively with the surface area. This is indicative of the fact that it is the surface chemistry rather than the bulk property that is dominant in the hybrid. However, the hybrid agglomerate with an increase in temperature by so reducing the effective adsorption capacity of the adsorbent.

4. Conclusion

Single molecular pectin-starch magnetite nanoparticles have been synthesized. The efficiency of the magnetite nanoparticle in removing methylene blue dye from an aqueous solution has been investigated. Results indicate that adsorption is pH and temperature dependent. The efficiency of the

Table 10: Influence of temperature pyrolysis on methylene blue adsorption of composite.

Sample	Initial conc. of dye	Final conc. of dye	% absorbance	% S.D.	% error
MV002_NP (60°C)	25	13.832	44.70	6.08	13.60
MV002 (180°C)	25	12.11	36.94	0.37	1.00

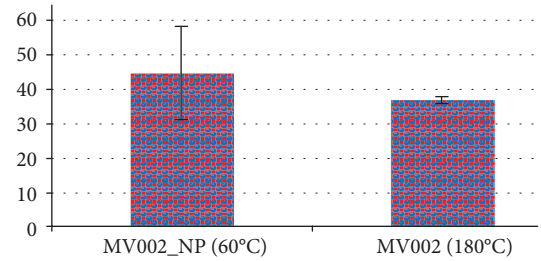

Figure 11: Bar charts showing the influence of temperature pyrolysis on methylene blue adsorption of composite.

absorbent increased with temperature though the hybrid decomposes to the magnetite at temperatures between 250°C and 550°C.

The developed pectin-starch magnetite hybrid not only has demonstrated higher adsorption efficiency especially at a low polymer concentration and starch-pectin ratio of 0.50 at ambient temperature but also has shown additional benefits like ease of synthesis, easy recovery, absence of secondary pollutants, cost-effectiveness, and environmental friendliness. It can be concluded to be a promising advanced adsorbent in environmental pollution cleanup.

Data Availability

All data used to support the findings of this study are included within the article.

Conflicts of Interest

There is no conflict of interest.

References

[1] Z. Carmen and S. Daniela, *Textile Organic Dyes Characteristics, Polluting Effects and Separation/Elimination Procedures from Industrial Effluents – A Critical Overview*, IntechOpen, 2012.

[2] A. P. Wanyama, B. Kiremire, J. E. S. Murumu, and H. Tumusiime, "Toxicological characterization of crude dye extracts derived from Albizia coriaria, Morinda lucida and V itellaria paradoxa selected dye - yielding plants in Uganda," *International Journal of Natural Products Research*, vol. 1, no. 2, pp. 16–20, 2012.

[3] S. Sharma, Kalpana, Arti et al., "Toxicity Assessment of Textile Dye Wastewater Using Swiss Albino Rats," *Australasian Journal of Ecotoxicology*, vol. 13, pp. 81–85, 2007.

[4] E. O. Oyelude and U. R. Owusu, "Adsorption of methylene blue from aqueous solution using acid modified *Calotropis Procera* leaf powder," *Journal of Applied Science and Environmental Sanitation*, vol. 6, no. 4, pp. 477–484, 2011.

[5] J.-L. Gong, X.-Y. Wang, G.-M. Zeng et al., "Copper (II) removal by pectin–iron oxide magnetic nanocomposite adsorbent," *Chemical Engineering Journal*, vol. 185-186, pp. 100–107, 2012.

[6] H. Tavallali and A. Daneshyar, "Modified iron oxide nanoparticles as solid phase extractor for spectrophotometric determination and separation of muroxide," *International Journal of ChemTech Research*, vol. 4, no. 3, pp. 1170–1173, 2012.

[7] A. O. Okewale, B. R. Etuk, and P. K. Igbokwe, "Comparative studies on some starchy adsorbents for the uptake of water from ethanol – water mixtures," *International Journal of Engineering & Technology*, vol. 11, no. 5, 2010.

[8] A. Tiwari and P. Kathane, *Superparamagnetic PVA-alginate microspheres as adsorbent for Cu^{2+} ions removal from aqueous systems*, International Science Congress Association, 2013.

[9] Y. Habibi, L. A. Lucia, and O. J. Rojas, "Cellulose nanocrystals: "chemistry, self-assembly, and applications"," *Chemical Reviews*, vol. 110, no. 6, pp. 3479–3500, 2010.

[10] S. Lin, C. C. Akoh, and A. E. Reynolds, "Determination of optimal conditions for selected adsorbent combinations to recover used frying oils," *Journal of the American Oil Chemists' Society*, vol. 76, no. 6, pp. 739–744, 1999.

[11] D. Le Corre, J. Bras, and A. Dufresne, "Starch nanoparticles: a review," *Biomacromolecules*, vol. 11, no. 5, pp. 1139–1153, 2010.

[12] J. Fresnais, M. Yan, J. Courtois, T. Bostelmann, A. Bée, and J.-F. Berret, "Poly(acrylic acid)-coated iron oxide nanoparticles: quantitative evaluation of the coating properties and applications for the removal of a pollutant dye," *Journal of Colloid and Interface Science*, vol. 395, pp. 24–30, 2013.

[13] S. F. Chin, S. C. Pang, and C. H. Tan, "Green synthesis of magnetite nanoparticles (via thermal decomposition method) with controllable size and shape," *Journal of Materials and Environmental Science*, vol. 2, no. 3, pp. 299–302, 2011.

[14] F.-T. J. Ngenefeme, N. J. Eko, Y. D. Mbom, N. D. Tantoh, and K. W. M. Rui, "A one pot green synthesis and characterisation of iron oxide-pectin hybrid nanocomposite," *Open Journal of Composite Materials*, vol. 3, no. 2, pp. 30–37, 2013.

[15] C. Kaewprasit, E. Hequet, N. Abidi, and J. P. Gourmont, *The Journal of Cotton Science*, vol. 2, pp. 164–173, 1998.

[16] B. Min, J. Lim, S. Ko, K.-G. Lee, S. H. Lee, and S. Lee, *Bioresource Technology*, vol. 102, no. 4, pp. 3855–3860, 2011.

[17] J. Sun, S. Zhou, P. Hou et al., "Synthesis and characterization of biocompatible Fe_3O_4 nanoparticles," *Journal of Biomedical Materials Research Part A*, vol. 80A, no. 2, pp. 333–341, 2007.

[18] R. K. Mishra, A. Anis, S. Mondal, M. Dutt, and A. K. Banthia, "Reparation and characterization of amidated pectin based polymer electrolyte membranes," *Chinese Journal of Polymer Science*, vol. 27, no. 5, pp. 639–646, 2009.

[19] M. Timko, P. Kop£anský, M. Antalik et al., "Magnetism - Magnetic properties of matter Poznan," in *European Conference of Physics and Magnetism*, Poland, 2011.